

NJC

Accepted Manuscript



This is an *Accepted Manuscript*, which has been through the Royal Society of Chemistry peer review process and has been accepted for publication.

Accepted Manuscripts are published online shortly after acceptance, before technical editing, formatting and proof reading. Using this free service, authors can make their results available to the community, in citable form, before we publish the edited article. We will replace this *Accepted Manuscript* with the edited and formatted *Advance Article* as soon as it is available.

You can find more information about *Accepted Manuscripts* in the [Information for Authors](#).

Please note that technical editing may introduce minor changes to the text and/or graphics, which may alter content. The journal's standard [Terms & Conditions](#) and the [Ethical guidelines](#) still apply. In no event shall the Royal Society of Chemistry be held responsible for any errors or omissions in this *Accepted Manuscript* or any consequences arising from the use of any information it contains.



www.rsc.org/njc

11/14

Carbonyl Migration from Phosphorus to the Metal in Binuclear Phosphaketonyl Metal Carbonyl Complexes to Give Bridging Diphosphido Complexes

Wenjun Lü,^a Chaoyang Wang,^a Qiong Luo,^{*a} Qian-shu Li,^a Yaoming Xie,^b
R. Bruce King,^{*a,b} and Henry F. Schaefer III^b

^a*MOE Key Laboratory of Theoretical Environmental Chemistry, Center for Computational Quantum Chemistry, South China Normal University, Guangzhou 510631, P. R. China*

^b*Department of Chemistry and Center for Computational Chemistry, University of Georgia, Athens, Georgia 30602, USA*

Abstract

Alkali metal salts of the 2-phosphaethynolate anion PCO^- synthesized from reactions of CO with NaPH_2 or K_3P_7 have recently become available in quantities for the synthesis of transition metal complexes of the potentially ambidentate PCO ligand (*Angew. Chem. Int. Ed.*, **2013**, 38, 10064). This is exemplified by the recently reported rhenium carbonyl complex $(\text{triphos})\text{Re}(\text{CO})_2(\text{PCO})$ ($\text{triphos} = \text{MeP}(\text{CH}_2\text{PPh}_2)_3$). Density functional theory studies on the related manganese carbonyl complexes $\text{Mn}(\text{CO})_n(\text{PCO})$ ($n = 5, 4, 3$) and $\text{Mn}_2(\text{CO})_n(\text{PCO})_2$ ($n = 8, 7, 6, 5$) are now reported. For the binuclear systems the low-energy $\text{Mn}_2(\text{CO})_8(\text{PCO})_2$ structures are singlet spin state structures having two bridging P-bonded phosphaketonyl μ -PCO ligands without a direct Mn–Mn bond. Carbonyl loss from $\text{Mn}_2(\text{CO})_8(\mu\text{-PCO})_2$ is predicted to lead to migration of CO groups from phosphorus to manganese resulting in $\text{Mn}_2(\text{CO})_{n+2}(\mu\text{-P}_2)$ structures with bridging diphosphido groups as the lowest energy $\text{Mn}_2(\text{CO})_n(\text{PCO})_2$ isomers ($n = 7, 6, 5$). Isomeric $\text{Mn}_2(\text{CO})_6(\text{PCO})_2$ structures with dihapto bridging η^2 - μ -PCO ligands at ~ 30 kcal/mol above the global minimum are also found representing intermediates in the migration of CO groups from phosphorus to manganese. For the mononuclear systems the P-bonded $\text{Mn}(\text{CO})_n(\text{PCO})$ ($n = 5, 4$) phosphaketonyl structures are found to lie 20 to 28 kcal mol⁻¹ in energy below the isomeric O-bonded $\text{Mn}(\text{CO})_n(\text{PCO})$ phosphaethynoxy isomers consistent with previously reported results by Grützmacher and coworkers on $\text{R}_3\text{E}(\text{PCO})/\text{R}_3\text{E}(\text{OCP})$ systems ($\text{R} = \text{iPr}, \text{Ph}$; $\text{E} = \text{Si}, \text{Sn}, \text{Ge}, \text{Pb}$). The lowest energy structure for the tricarbonyl $\text{Mn}(\text{CO})_3(\text{PCO})$ is a singlet structure with an unusual trihapto η^3 -PCO ligand. However, higher energy isomeric $\text{Mn}(\text{CO})_3(\text{PCO})$ structures with P-bonded phosphaketonyl or O-bonded phosphaethynoxy ligands and tetrahedral Mn coordination are also found.

1. Introduction

One of the simplest inorganic phosphorus ligands is the 2-phosphaethynolate anion PCO^- , which is the phosphorus analogue of the much more familiar isocyanate anion NCO^- . However, until recently the development of the coordination chemistry of the 2-phosphaethynolate ligand has been limited by difficulties in its synthesis. In 1992 Becker and coworkers¹ first reported the 2-phosphaethynolate anion (PCO^-) as a product from the reaction of $\text{LiP}(\text{SiMe}_3)_2$ with dimethylcarbonate. However, the yields from this reaction were too low to make the PCO^- anion sufficiently accessible as a reagent for the synthesis of coordination compounds. The key breakthrough in making the PCO^- available enough for study of its chemistry occurred only in 2011 when Grützmacher and coworkers² found that heating NaPH_2 in dimethoxyethane solution with CO under pressure cleanly gave the sodium salt NaOCP as its dimethoxyethane solvate. This sodium salt was used to prepare the rhenium carbonyl complex $(\text{triphos})\text{Re}(\text{CO})_2(\text{PCO})$ ($\text{triphos} = \text{MeP}(\text{CH}_2\text{PPh}_2)_3$) by a simple metathesis reaction in tetrahydrofuran solution.³ In addition NaOCP has been shown to be a useful reagent for the synthesis of phosphorus heterocycles^{4,5} and unusual phosphorus-based stable free radicals.⁶ Subsequently a more convenient synthesis of the PCO^- anion as its potassium salt was discovered by Jupp and Goicoechea⁷ using the reaction of a dimethylformamide solution of K_3P_7 with CO at atmospheric pressure in the presence of [18]-crown-6. A very recently reported synthesis of NaOCP by Grützmacher et al. from red phosphorus, sodium, and ethylene carbonate is still more convenient since the use of CO as a reagent is avoided.⁴

The PCO^- ligand is an ambidentate ligand⁸ analogous to the (iso)cyanate ligand, NCO^- , that can bond to a metal atom either through its phosphorus atom as a phosphaketanyl ligand or through its oxygen atom as a 2-phosphaethynoxy ligand. The recently reported syntheses of salts of the PCO^- anion use reactions of CO with phosphorus anions, which, at least formally, can be sources of the P^- monoanion unknown except in the gas phase. Thus the NaPH_2 used in the Grützmacher synthesis² of solvated NaOCP can generate “NaP” by loss of H_2 . Use of K_3P_7 as a source of P^- in the Goicoechea synthesis⁷ of solvated KOCP is more complicated but is seen to lead to the polyphosphide anions P_{16}^{2-} and P_{21}^{3-} as by-products. The success in such syntheses of PCO^- salts by carbonylation of reagents generating P^- fragments suggests the possibility of reversing such reactions by using transition metal PCO complexes to generate novel transition metal phosphide complexes. In order to explore this possibility we have undertaken a theoretical study of the manganese carbonyl complexes $\text{Mn}(\text{CO})_n(\text{PCO})$ ($n = 5, 4, 3$) and $\text{Mn}_2(\text{CO})_n(\text{PCO})_2$ ($n = 8, 7, 6, 5$). We chose manganese carbonyl

derivatives for our initial studies in this area because of their relationship to the rhenium carbonyl derivative (triphos)Re(CO)₂(PCO) that has been synthesized and structurally characterized by X-ray crystallography.³ Our results, reported in this paper, predict the generation of isomeric phosphide and diphosphide Mn₂(CO)_{n+2}P₂ complexes having six to nine terminal CO groups in the unsaturated Mn₂(CO)_n(PCO)₂ (*n* = 7, 6, 5) systems. In addition, Mn₂(CO)₆(PCO)₂ structures containing three-electron donor bridging η^2 - μ -PCO groups have been discovered. Such structures are plausible intermediates in the migration of CO from phosphorus in a PCO ligand to a metal atom.

2. Theoretical Methods

Electron correlation effects were considered by using density functional theory (DFT) methods, which have evolved as a practical and effective computational tool, especially for organometallic compounds.^{9,10,11,12,13,14,15} Two DFT methods (B3LYP and BP86) were used in this study. The B3LYP method is the hybrid HF/DFT method using a combination of the three-parameter Becke functional (B3)¹⁶ with the Lee–Yang–Parr (LYP) generalized gradient correlation functional.¹⁷ The BP86 method combines Becke's 1988 exchange functional (B)¹⁸ with Perdew's 1986 gradient corrected correlation functional (P86).¹⁹

In this work all computations were performed using double- ζ plus polarization (DZP) basis sets. For carbon, oxygen and phosphorus, these DZP basis sets are obtained by adding one set of pure spherical harmonic d functions with orbital exponents $\alpha_d(\text{C}) = 0.75$, $\alpha_d(\text{O}) = 0.85$, and $\alpha_d(\text{P}) = 0.60$ to the standard Huzinaga–Dunning contracted DZ sets.^{20,21} The loosely contracted DZP basis set for manganese is the Wachters primitive set²² augmented by two sets of p functions and one set of d functions and contracted following Hood, Pitzer, and Schaefer,²³ and is designated as (14s11p6d/10s8p3d).²⁴

The geometries of all structures were fully optimized. Vibrational frequencies and their corresponding infrared intensities were determined analytically. All of the computations were carried out with the Gaussian 09 program,²⁵ exercising the fine integration grid option (75 radial shells, 302 angular points) for evaluating integrals numerically.²⁶ The finer (120, 974) grid was only used to check small imaginary vibrational frequencies.

The optimized structures are shown in Figures 1 to 6 and Tables 1 to 6. Structures are designated as **ab-cS** (or **ab-cT**), where **a** is the number of manganese atoms (the same as the number of PCO groups), **b** is the number of CO groups, and **c** orders the structures according to their relative energies by the B3LYP method. **S** and **T**

represent singlet and triplet spin state structures, respectively. Thus the lowest energy structure (singlet) of $\text{Mn}_2(\text{CO})_8(\text{PCO})_2$ is designated as **28-1S**.

3. Results

3.1. The mononuclear derivatives $\text{Mn}(\text{CO})_n(\text{PCO})$ ($n = 5, 4, 3$)

3.1.1 $\text{Mn}(\text{CO})_5(\text{PCO})$. Two $\text{Mn}(\text{CO})_5(\text{PCO})$ structures have been optimized, namely **15-1S** and **15-2S** (Figure 1 and Table 1). The global minimum **15-1S** is a C_s singlet structure with approximate octahedral Mn coordination, similar to that in the experimentally known $\text{HMn}(\text{CO})_5$.^{27,28,29} The PCO group is a monohapto η^1 -PCO phosphaketonyl ligand coordinated to the Mn atom through the phosphorus atom with a strongly bent Mn–P–C angle of 98.3° (B3LYP) or 98.0° (BP86). This compares with an experimental Re–P–C angle of 92.6° determined by X-ray crystallography in the related Grützmacher complex $(\text{triphos})\text{Re}(\text{CO})_2(\text{PCO})$.³ The strongly bent Mn–P–C angle in **15-1S** indicates a stereochemically active lone pair on the phosphorus atom, implying that the neutral PCO ligand is a one-electron donor.

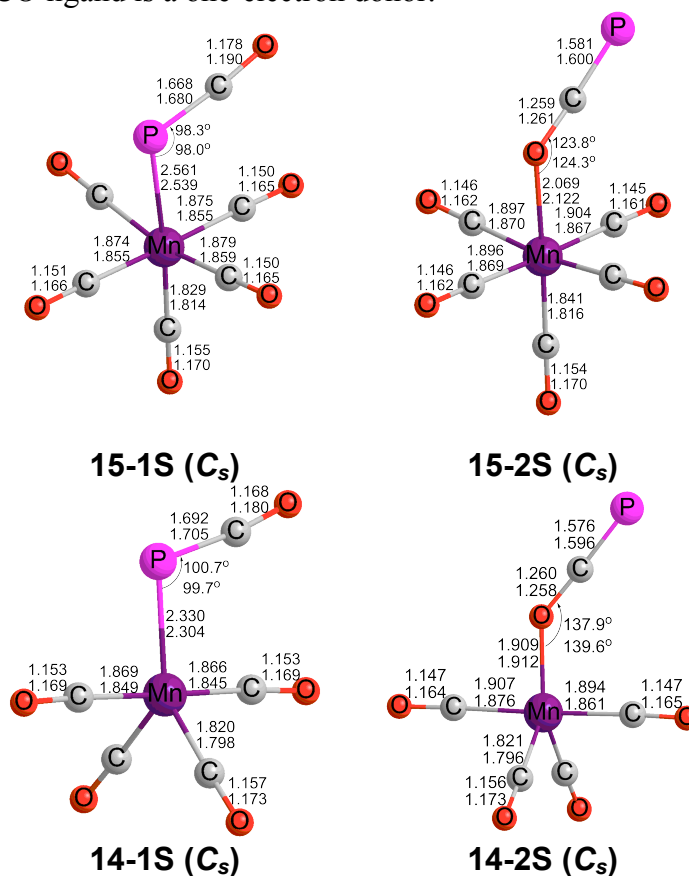


Figure 1. The optimized $\text{Mn}(\text{CO})_5(\text{PCO})$ and $\text{Mn}(\text{CO})_4(\text{PCO})$ structures. Bond distances are given in Å with the B3LYP values on top and the BP86 values on the bottom.

Table 1 Total energies (E in Hartree) and relative energies with and without ZPVE corrections (ΔE and ΔE_{ZPVE} in kcal mol⁻¹ for the Mn(CO)₅(PCO) and Mn(CO)₄(PCO) structures. None of these structures has any imaginary vibrational frequencies.

		15-1S (<i>C_s</i>)	15-2S (<i>C_s</i>)	14-1S (<i>C_s</i>)	14-2S (<i>C_s</i>)
B3LYP	-E	2172.56143	2172.52527	2059.19129	2059.15984
	ΔE	0.0	22.7	0.0	19.7
	ΔE_{ZPVE}	0.0	22.4	0.0	19.5
BP86	-E	2172.82339	2172.77861	2059.40542	2059.40962
	ΔE	0.0	28.1	0.0	24.2
	ΔE_{ZPVE}	0.0	27.7	0.0	24.0

The isomeric O-bonded singlet phosphaehtoxy Mn(CO)₅(OCP) structure **15-2S** was also optimized. However, it was found to be a high energy structure, lying 22.7 kcal mol⁻¹ (B3LYP) or 28.1 kcal mol⁻¹ (BP86) above **15-1S** (Figure 1 and Table 1). Thus phosphorus coordination of the PCO ligand appears to be greatly preferred over oxygen coordination, at least in metal carbonyl complexes. The predicted M–O–C angle in the phosphaehtoxy complex **15-2S** of 123.8° (B3LYP) or 124.3° (BP86) is not as sharply bent as the M–P–C angle in the phosphaketanyl complex **15-1S**. The neutral PCO ligand is a one-electron donor in both **15-1S** and **15-2S** thereby giving the Mn atoms the favored 18-electron configuration. Triplet states of Mn(CO)₅(PCO) lie more than 30 kcal mol⁻¹ in energy above **15-1S** and thus are not discussed in this paper.

3.1.2 Mn(CO)₄(PCO). Two low-lying singlet structures, namely **14-1S** and **14-2S**, were found for Mn(CO)₄(PCO) (Figure 1 and Table 1). Structure **14-1S** is a genuine minimum with *C_s* symmetry, which can be derived from the singlet Mn(CO)₅(PCO) phosphaketanyl structure **15-1S** by removal of the axial CO group with some distortion of the remaining four CO groups. The predicted Mn–P bond length of ~2.32 Å in structure **14-1S** is significantly shorter than the Mn–P bond length of ~2.55 Å in **15-1S**. The bent PCO group in **14-1S**, like that in **15-1S**, implies a stereochemically active lone pair on the phosphorus atom so that the PCO group in **14-1S**, considered as a neutral ligand, is a one-electron donor to give the Mn atom a 16-electron configuration. Structure **14-2S** is an isomeric O-bonded singlet phosphaehtoxy Mn(CO)₄(OCP) structure similar to **15-2S**, lying at the relatively high energy of 19.7 kcal mol⁻¹ (B3LYP) or 28.1 kcal mol⁻¹ (BP86) above **14-1S**. The M–O–C angle in **14-2S** of ~138° is larger than that of **15-2S**. The PCO ligand in **14-2S** is a one-electron donor to give the Mn atom a 16-electron configuration.

3.1.3 Mn(CO)₃(PCO). Two singlet state structures and one energetically competitive triplet state structure were found for Mn(CO)₃(PCO) (Figure 2 and Table 2). None of these structures has any imaginary vibrational frequencies. The lowest energy singlet

structure **13-1S** has an unprecedented trihapto η^3 -PCO group, as indicated by bonding Mn–O, Mn–C, and Mn–P distances of ~ 2.2 , ~ 2.0 , and ~ 2.4 Å, respectively. Such a neutral PCO ligand in **13-1S** is a three-electron donor, leading to a 16-electron configuration for the Mn atom. The C_{3v} tetrahedral $Mn(CO)_3(PCO)$ structure **13-2S** with an O-bonded PCO 2-phosphaethoxy group, lies 14.6 kcal mol $^{-1}$ (B3LYP) or 17.9 kcal mol $^{-1}$ (BP86) above **13-1S**. The linear PCO ligand with the O atom linking to the Mn atom is a three-electron donor to give the Mn atom a 16-electron configuration. The triplet state $Mn(CO)_3(PCO)$ structure **13-1T**, lying 10.5 kcal mol $^{-1}$ (B3LYP) or 23.2 kcal mol $^{-1}$ (BP86) in energy above **13-1S**, has approximately square planar Mn coordination and a bent P-bonded phosphaketenyl ligand with a Mn–P–C angle of 101.3°. The Mn–P bond distance in **13-1T** is predicted to be 2.392 Å (B3LYP) or 2.345 Å (BP86), which is comparable to the Mn–P bond distance in **14-1S**. The bent PCO group is a one-electron donor, leading to a 14-electron configuration for the Mn atom.

Table 2. Total energies (E in Hartree), relative energies with and without ZPVE corrections (ΔE and ΔE_{ZPVE} in kcal mol $^{-1}$), and spin expectation values $\langle S^2 \rangle$ for the $Mn(CO)_3(PCO)$ structures. None of the structures has any imaginary vibrational frequencies.

		13-1S (C_s)	13-2S (C_{3v})	13-1T (C_s)
B3LYP	–E	1945.82001	1945.79678	1945.80328
	ΔE	0.0	14.6	10.5
	ΔE_{ZPVE}	0.0	14.5	9.6
	$\langle S^2 \rangle$	0.00	0.00	2.10
BP86	–E	1946.06906	1946.04051	1946.03211
	ΔE	0.0	17.9	23.2
	ΔE_{ZPVE}	0.0	17.9	22.2
	$\langle S^2 \rangle$	0.00	0.00	2.05

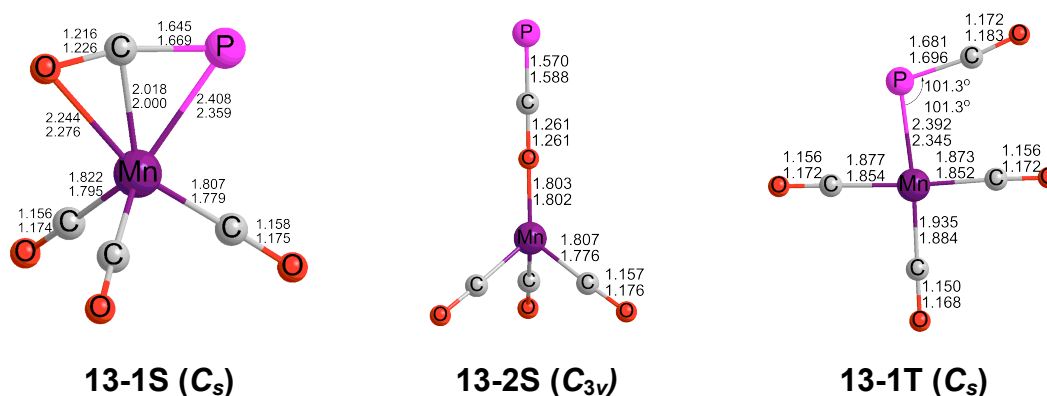


Figure 2. The optimized $Mn(CO)_3(PCO)$ structures. Bond distances are given in Å, with the B3LYP values on top and the BP86 values on the bottom.

3.2. Binuclear Derivatives

3.2.1 $Mn_2(CO)_8(PCO)_2$. Three singlet structures **28-1S**, **28-2S**, and **28-3S** were found having energies within 20 kcal mol⁻¹ (Figure 3 and Table 3). All of these $Mn_2(CO)_8(PCO)_2$ structures are genuine minima. The global minimum **28-1S** (C_{2h}) has two three-electron donor bridging phosphaketanyl μ -PCO ligands bonded to the manganese atoms solely through the phosphorus atoms. The geometry of **28-1S** is similar to $H_2Mn_2(CO)_8$ predicted in a previous DFT study,²⁹ and also similar to $H_2Re_2(CO)_8$ observed by X-ray crystallography.^{30,31} The C_{2v} structure **28-2S**, lying only 0.4 kcal mol⁻¹ (B3LYP or BP86) in energy above **28-1S**, is a *cis* stereoisomer with different PCO orientations. This small energy difference suggests fluxionality for the $Mn_2(CO)_8(PCO)_2$ system. Each manganese atom in **28-1S** and **28-2S** has octahedral coordination. The Mn...Mn distances of ~ 3.8 Å in these two structures are nearly 1 Å longer than the Mn–Mn single bond distance in $Mn_2(CO)_{10}$ of 2.92 Å³² or 2.895 Å,³³ determined by X-ray crystallography. Thus, there appear to be no direct Mn–Mn bonds in these $Mn_2(CO)_8(PCO)_2$ structures. Since each of the bridging μ -PCO ligands is a three-electron donor, each manganese atom in **28-1S** and **28-2S** has the favored 18-electron configuration even without an Mn–Mn bond.

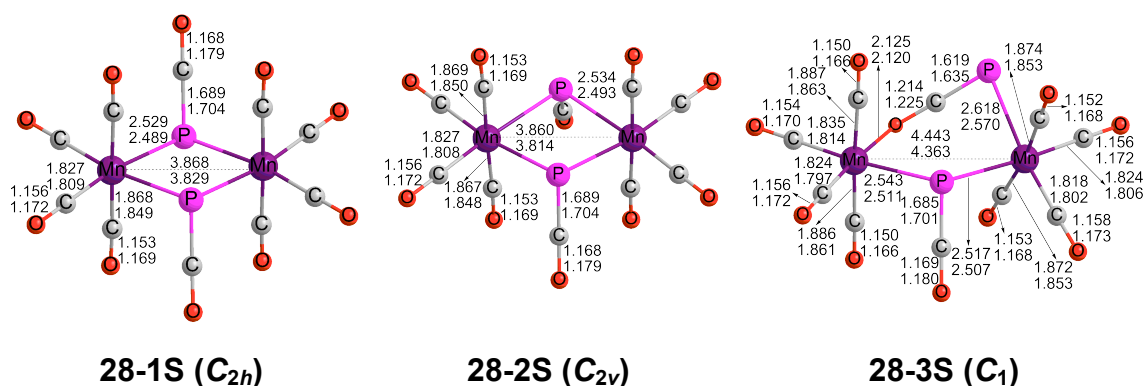


Figure 3. The optimized $Mn_2(CO)_8(PCO)_2$ structures. Bond distances are given in Å, with the B3LYP values on top and the BP86 values on the bottom.

An isomeric $Mn_2(CO)_8(PCO)_2$ structure **28-3S**, lying 11.4 kcal mol⁻¹ (B3LYP) or 16.4 kcal mol⁻¹ (BP86) in energy above **28-1S**, has two three-electron donor bridging μ -PCO phosphaketanyl μ -PCO ligands like **28-1S** and **28-2S** (Figure 3 and Table 3). However, one of these bridging ligands is a three-electron donor end-to-end dihapto η^2 - μ -PCO ligand bonded to one Mn atom through the phosphorus atom (Mn–P distance of ~ 2.6 Å) and to the other Mn atom through the oxygen atom (Mn–O distance of ~ 2.1 Å).

The other bridging phosphaketenyl ligand in **28-3S** is a three-electron donor monohapto bridging μ -PCO ligand similar to the μ -PCO ligands in **28-1S** and **28-2S**. The long Mn \cdots Mn distance of ~ 4.4 Å in **28-3S** implies the absence of a direct Mn–Mn bond. Nevertheless, each Mn atom in **28-3S** has the favored 18-electron configuration. Triplet spin states of $\text{Mn}_2(\text{CO})_8(\text{PCO})_2$ are found to lie at least 20 kcal mol $^{-1}$ above the global minimum **28-1S** and thus are not discussed in this paper.

Table 3. Total energies (E in Hartree) and relative energies with and without ZPVE corrections (ΔE and ΔE_{ZPVE} in kcal mol $^{-1}$), for the $\text{Mn}_2(\text{CO})_8(\text{PCO})_2$ structures. None of these structures has any imaginary vibrational frequencies.

		28-1S (C_{2h})	28-2S (C_{2v})	28-3S (C_1)
B3LYP	–E	4118.43386	4118.43331	4118.41564
	ΔE	0.0	0.4	11.4
	ΔE_{ZPVE}	0.0	0.3	11.4
BP86	–E	4118.95341	4118.95271	4118.92723
	ΔE	0.0	0.4	16.4
	ΔE_{ZPVE}	0.0	1.4	16.5

3.2.2 $\text{Mn}_2(\text{CO})_7(\text{PCO})_2$. The two lowest energy structures of stoichiometry $\text{Mn}_2(\text{CO})_7(\text{PCO})_2$ are the $\text{Mn}_2(\text{CO})_9\text{P}_2$ isomers **27-1S** and **27-2S** (Figure 4 and Table 4). In these two structures the carbonyls in the PCO groups have migrated from the phosphorus atoms to the two manganese atoms, leaving a coupled P_2 fragment bridging the two manganese atoms. Neither structure has any imaginary vibrational frequencies. The lowest energy $\text{Mn}_2(\text{CO})_9\text{P}_2$ structure **27-1S** (C_s) has an $\eta^3\text{-P}_2$ group with a P=P distance of 1.991 Å (B3LYP) or 2.002 Å (BP86) corresponding to a formal double bond. The long Mn \cdots Mn distance (> 4.7 Å) in **27-1S** implies the absence of a direct bond. Since the bridging $\eta^3\text{-P}_2$ ligand is a four-electron donor with a lone pair remaining on the phosphorus atom bonded to only a single manganese atom, each manganese atom in **27-1S** has the favored 18-electron configuration. The $\text{Mn}_2(\text{CO})_9\text{P}_2$ structure **27-2S**, lying 6.6 kcal mol $^{-1}$ (B3LYP) or 5.2 kcal mol $^{-1}$ (BP86) in energy above **27-1S**, has a bridging end-to-end P_2 group. The P=P distance of 1.991 Å (B3LYP) or 2.005 Å (BP86) in **27-2S** corresponds to a formal double bond. The Mn–P distance of 2.552 Å (B3LYP) or 2.531 Å (BP86) to the $\text{Mn}(\text{CO})_5$ group corresponds to a formal single bond. The much shorter Mn=P distance of 2.113 Å (B3LYP) or 2.107 Å (BP86) to the $\text{Mn}(\text{CO})_4$ corresponds to a formal double bond. This gives each Mn atom the favored 18-electron configuration if the $\text{Mn}(\text{CO})_4$ manganese bears a formal negative charge and the phosphorus atom bonded to the $\text{Mn}(\text{CO})_4$ group bears a formal positive charge.

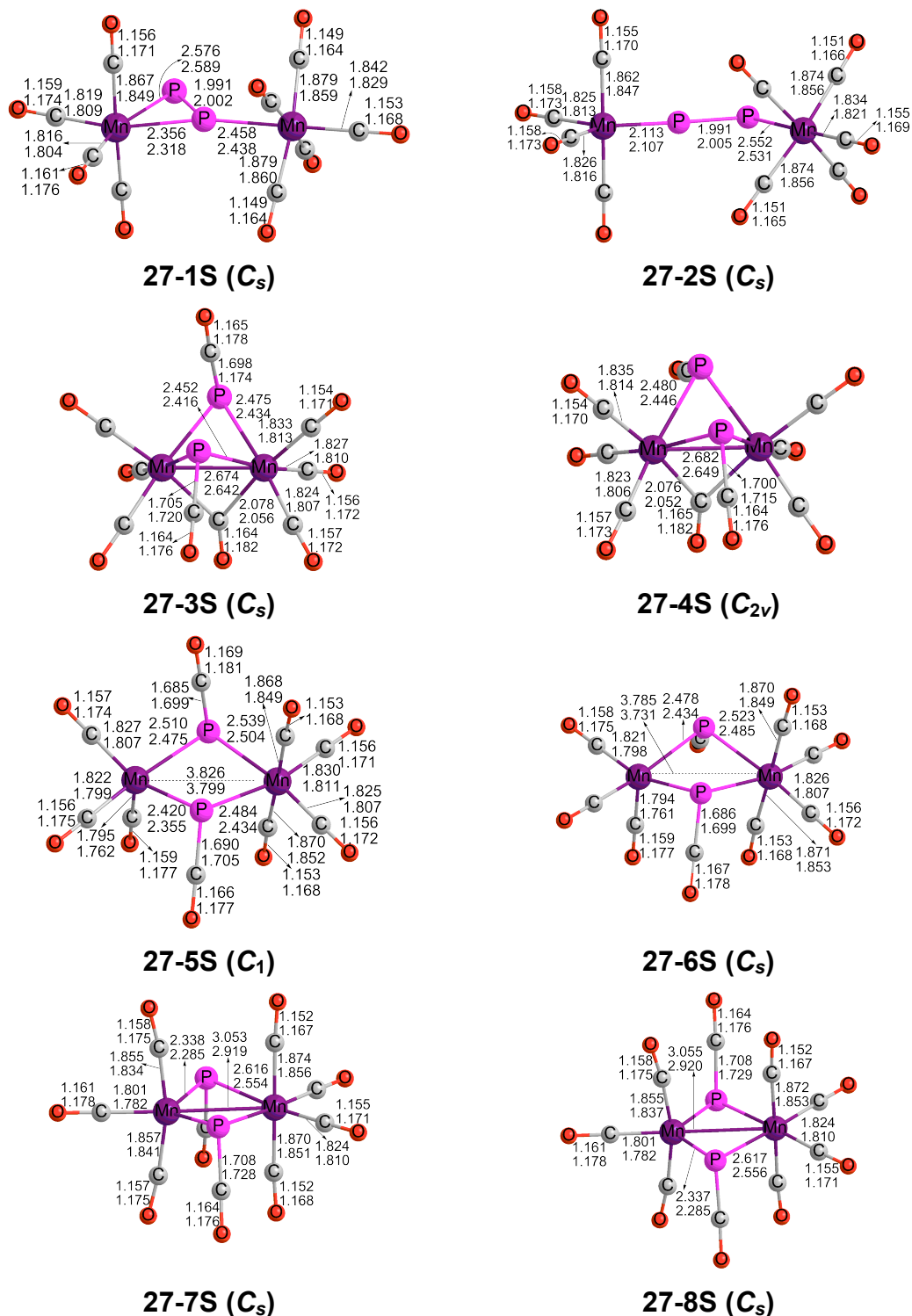


Figure 4. The optimized $Mn_2(CO)_7(PCO)_2$ structures. Bond distances are given in Å, with the B3LYP values on top and the BP86 values on the bottom.

Table 4. Total energies (E in Hartree) and relative energies with and without ZPVE corrections (ΔE and ΔE_{ZPVE} in kcal mol⁻¹) for the Mn₂(CO)₇(PCO)₂ structures. None of the structures has any imaginary vibrational frequencies.

		27-1S (<i>C_s</i>)	27-2S (<i>C_s</i>)	27-3S (<i>C_s</i>)	27-4S (<i>C_{2v}</i>)
B3LYP	-E	4005.08012	4005.06961	4005.05775	4005.05824
	ΔE	0.0	6.6	14.0	13.7
	ΔE_{ZPVE}	0.0	6.5	13.8	13.6
BP86	-E	4005.59327	4005.58491	4005.58237	4005.58181
	ΔE	0.0	5.2	6.8	7.2
	ΔE_{ZPVE}	0.0	5.2	6.7	7.1
		27-5S (<i>C₁</i>)	27-6S (<i>C_s</i>)	27-7S (<i>C_s</i>)	27-8S (<i>C_s</i>)
B3LYP	-E	4005.05078	4005.05106	4005.04285	4005.04288
	ΔE	18.4	18.2	23.4	23.4
	ΔE_{ZPVE}	18.0	17.9	23.0	23.0
BP86	-E	4005.56098	4005.56081	4005.56007	4005.55997
	ΔE	20.3	20.4	20.8	20.9
	ΔE_{ZPVE}	20.0	20.1	20.5	20.6

The Mn₂(CO)₇(PCO)₂ structures **27-3S** (*C_s*) and **27-4S** (*C_{2v}*) are a *trans-cis* stereoisomer pair, which are degenerate in energy within 0.4 kcal mol⁻¹ (Figure 4 and Table 4). These structures lie ~14 kcal mol⁻¹ (B3LYP) or ~7 kcal mol⁻¹ (BP86) in energy above **27-1S**. Both **27-3S** and **27-4S** have two three-electron donor P-bonded bridging μ -PCO groups similar to those in **28-1S** and **28-2S** (Figure 3) as well as one bridging μ -CO group and six terminal CO groups. The Mn–Mn bond distances of 2.674 Å (B3LYP) or 2.642 Å (BP86) in **27-3S** and 2.682 Å (B3LYP) or 2.649 Å (BP86) in **27-4S** can correspond to the formal Mn–Mn single bond needed to give each Mn atom in **27-3S** and **27-4S** the favored 18-electron configuration.

The Mn₂(CO)₇(PCO)₂ structures **27-5S** (*C₁*) and **27-6S** (*C_s*) are another *trans-cis* stereoisomer pair with two bridging μ -PCO groups and seven terminal CO groups. Structures **27-5S** and **27-6S** are almost degenerate in energy within 0.2 kcal mol⁻¹ and lie ~18 kcal mol⁻¹ (B3LYP) or ~20 kcal mol⁻¹ (BP86) above **27-1S**. The long Mn...Mn distances in **27-5S** and **27-6S** of ~3.80 Å indicate lack of direct Mn–Mn bonding. Thus, in **27-5S** and **27-6S**, the Mn atom bearing four CO groups has the favored 18-electron configuration, while the Mn atom bearing three CO groups has only a 16-electron configuration. Structures **27-5S** and **27-6S** can be derived from structures **28-1S** and **28-2S** by removal of one axial carbonyl group, respectively, thereby leaving a hole in the octahedral coordination of the Mn atoms with the 16-electron configuration.

The $\text{Mn}_2(\text{CO})_7(\text{PCO})_2$ structures **27-7S** and **27-8S** are also a *cis-trans* stereoisomer pair with two bridging μ -PCO groups and seven terminal CO groups (Figure 4 and Table 4). They are degenerate in energy within $0.1 \text{ kcal mol}^{-1}$, lying $\sim 23 \text{ kcal mol}^{-1}$ (B3LYP) or $\sim 21 \text{ kcal mol}^{-1}$ (BP86) above **27-1S**. The Mn–Mn distances of 3.053 \AA (B3LYP) or 2.919 \AA (BP86) for **27-7S** and 3.055 \AA (B3LYP) or 2.920 \AA (BP86) **27-8S** can correspond to long single bonds from the $\text{Mn}(\text{CO})_4$ manganese to the $\text{Mn}(\text{CO})_3$ manganese. This gives each Mn atom the favored 18-electron configuration.

3.2.3 $\text{Mn}_2(\text{CO})_6(\text{PCO})_2$. Similar to $\text{Mn}_2(\text{CO})_7(\text{PCO})_2$, the six lowest energy $\text{Mn}_2(\text{CO})_6(\text{PCO})_2$ structures **26-1S**, **26-2S**, **26-3S**, **26-1T**, **26-4S**, and **26-2T** are essentially $\text{Mn}_2(\text{CO})_8(\mu\text{-P}_2)$ structures with bridging diphosphido ligands (Figure 5 and Table 5). Structures **26-1S** and **26-2S** have similar geometries (only with different relative CO positions) and similar relative energies within $1.0 \text{ kcal mol}^{-1}$. Both **26-1S** (C_2) and **26-2S** (C_s) have a four-electron donor bridging $\mu\text{-P}_2$ ligand with Mn–P distances of $\sim 2.4 \text{ \AA}$ as well as eight terminal CO groups. The Mn–Mn distances of $\sim 2.8 \text{ \AA}$ suggest formal single Mn–Mn bonds, thereby giving each Mn atom the favored 18-electron configuration. Structure **26-3S**, lying $3.5 \text{ kcal mol}^{-1}$ (B3LYP) or $16.4 \text{ kcal mol}^{-1}$ (BP86) above **26-1S**, has a P_2 group bridging the two Mn atoms. The long Mn \cdots Mn distance ($> 4.2 \text{ \AA}$) in **26-3S** implies the absence of a direct Mn–Mn bond.

The triplet $\text{Mn}_2(\text{CO})_6(\mu\text{-P}_2)$ structure **26-1T**, lying $15.7 \text{ kcal mol}^{-1}$ (B3LYP) or $26.2 \text{ kcal mol}^{-1}$ (BP86) in energy above **26-1S**, has similar geometry to **26-1S** with the P_2 group bridging the two Mn atoms (Figure 5 and Table 5). The Mn–P and P–P distances in **26-1T** are $\sim 2.4 \text{ \AA}$ and $\sim 2.2 \text{ \AA}$, respectively. The very long Mn \cdots Mn distance in **26-1T** of $\sim 4.1 \text{ \AA}$ indicates lack of direct Mn–Mn bonding thereby giving each Mn atom the 17-electron configuration, consistent with a binuclear triplet spin state structure.

The $\text{Mn}_2(\text{CO})_6(\mu\text{-P}_2)$ structure **26-4S**, lying $17.9 \text{ kcal mol}^{-1}$ (B3LYP) or $27.8 \text{ kcal mol}^{-1}$ (BP86) in energy above **26-1S**, has an end-to-end P_2 group bridging the two Mn atoms (Figure 5 and Table 5). Structure **26-4S** has one tiny imaginary vibrational frequency, but this becomes real when a finer integration grid (120, 974) is used. Structure **26-4S** can be derived from **27-2S** by loss of a CO group from the $\text{Mn}(\text{CO})_5$ unit. The Mn–P and P=P distances in **26-4S** are $\sim 2.1 \text{ \AA}$ and $\sim 2.0 \text{ \AA}$, respectively. The long Mn \cdots Mn distance ($> 6.0 \text{ \AA}$) in **26-4S** implies the absence of a direct Mn–Mn bond. The $\mu\text{-P}_2$ ligand has a formal P=P double bond and donates three electrons to each manganese atom. This gives each manganese atom the favored 18-electron configuration.

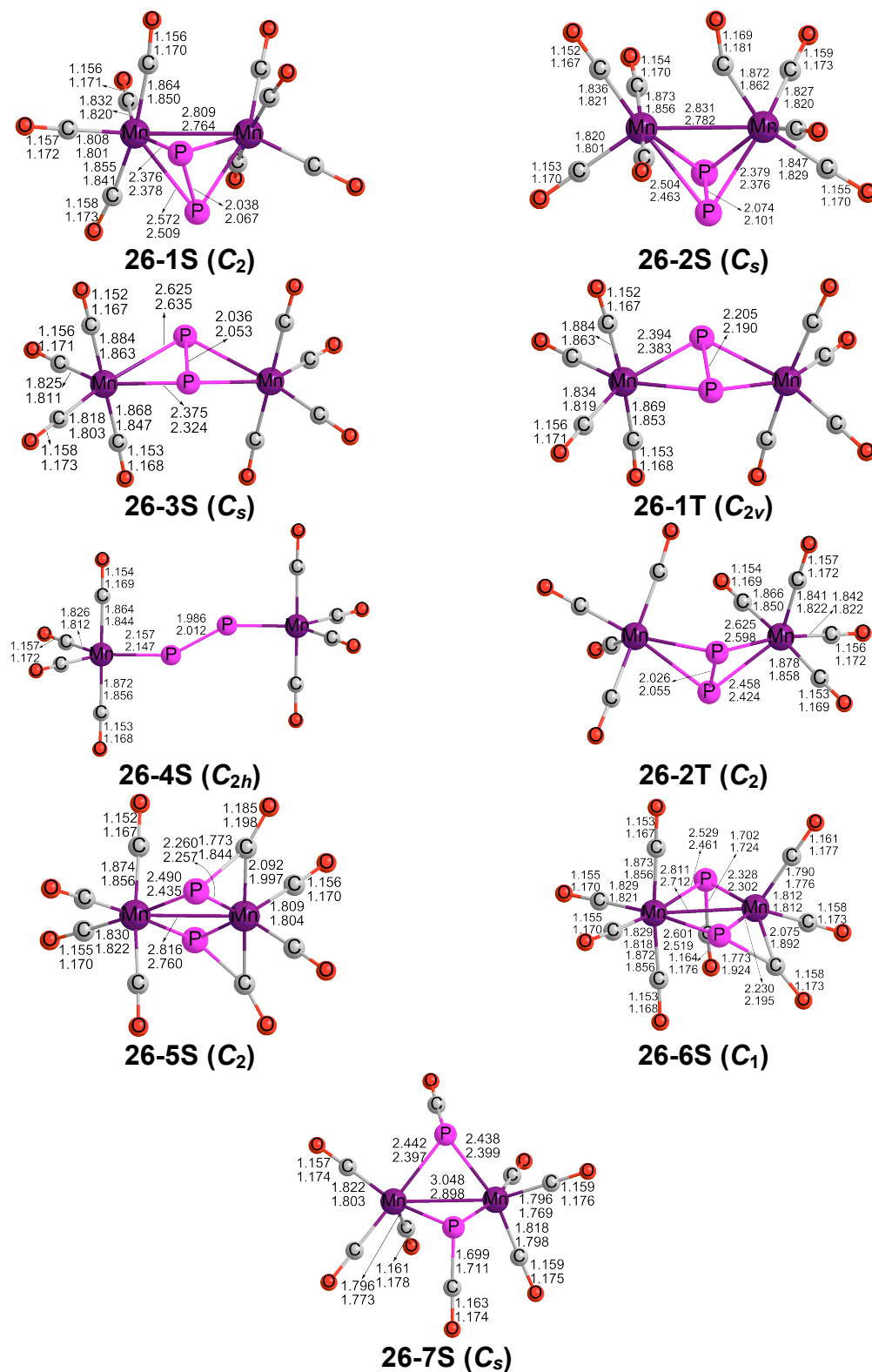


Figure 5. The optimized $\text{Mn}_2(\text{CO})_6(\text{PCO})_2$ structures. Bond distances are given in Å, with the B3LYP values on top and the BP86 values on the bottom.

Table 5. Total energies (E in Hartree), relative energies with and without ZPVE corrections (ΔE and ΔE_{ZPVE} in kcal mol⁻¹), numbers of imaginary vibrational frequencies (N_{img}), and spin expectation values $\langle S^2 \rangle$ for the Mn₂(CO)₆(PCO)₂ structures.

		26-1S (<i>C</i> ₂)	26-2S (<i>C</i> _s)	26-3S (<i>C</i> _s)	26-1T (<i>C</i> _{2v})	26-4S (<i>C</i> _{2h})
B3LYP	-E	3891.71697	3891.71857	3891.71135	3891.69195	3891.68847
	ΔE	0.0	-1.0	3.5	15.7	17.9
	ΔE_{ZPVE}	0.0	-0.9	2.9	14.6	17.2
	N_{img}	none	none	none	none	1(5.7i)
	$\langle S^2 \rangle$	0.00	0.00	0.00	2.06	0.00
BP86	-E	3892.24546	3892.24509	3892.21939	3892.20378	-3892.20121
	ΔE	0.0	0.2	16.4	26.2	27.8
	ΔE_{ZPVE}	0.0	0.3	15.9	25.2	27.1
	N_{img}	none	none	none	none	1(0.3i)
	$\langle S^2 \rangle$	0.00	0.00	0.00	2.02	0.00

		26-2T (<i>C</i> ₂)	26-5S (<i>C</i> ₂)	26-6S (<i>C</i> ₁)	26-7S (<i>C</i> _s)
B3LYP	-E	3891.69187	3891.66912	3891.66690	3891.67999
	ΔE	15.8	30.0	31.4	23.2
	ΔE_{ZPVE}	14.4	29.3	30.5	22.5
	N_{img}	none	none	none	none
	$\langle S^2 \rangle$	2.03	0.00	0.00	0.00
BP86	-E	3892.19927	3892.20182	3892.18906	3892.18602
	ΔE	29.0	27.4	35.4	37.3
	ΔE_{ZPVE}	27.8	26.9	34.5	36.6
	N_{img}	none	none	none	none
	$\langle S^2 \rangle$	2.01	0.00	0.00	0.00

The triplet Mn₂(CO)₆(μ -P₂) structure **26-2T**, lying 15.8 kcal mol⁻¹ (B3LYP) or 29.0 kcal mol⁻¹ (BP86) in energy above **26-1S**, has a similar structure to **26-1T** except for the positions of the CO groups (Figure 5 and Table 5). The bridging μ -P₂ group in **26-2T** is bonded to the two Mn atoms with Mn-P distances of 2.625 and 2.458 Å (B3LYP) or 2.598 and 2.424 Å (BP86). The long Mn...Mn distance (> 4.0 Å) in **26-2T** implies the absence of a direct Mn-Mn bond thereby giving each Mn atom the 17-electron configuration for a binuclear triplet.

Three low-lying Mn₂(CO)₆(PCO)₂ structures with intact PCO ligands were optimized, namely **26-5S**, **26-6S**, and **26-7S** (Figure 5 and Table 5). Although the BP86 method prefers energetically the structures with the normal bridging μ -PCO groups and

the B3LYP method prefers structures with dihapto bridging η^2 - μ -PCO ligands, these three structures have relative energies within 10 kcal mol⁻¹. The C₂ structure **26-5S**, lying ~30 kcal mol⁻¹ (B3LYP) or ~27 kcal mol⁻¹ (BP86) in energy above **26-1S**, has two three-electron donor bridging dihapto η^2 - μ -PCO ligands and six terminal CO groups. The η^2 - μ -PCO bridging ligands in structure **26-5S** are bonded to the “right” Mn atom (Figure 5) through both phosphorus and carbon atoms with a short Mn–C distance of ~2.0 Å and bonded to the “left” Mn atom only through the P atoms. The Mn–Mn distance of 2.816 Å (B3LYP) or 2.760 Å (BP86) in **26-5S** can be interpreted as a single bond, thereby giving the Mn atom bonded to four terminal CO groups (the “left” Mn atom in Figure 5) the favored 18-electron configuration but the other Mn atom only a 16-electron configuration.

The Mn₂(CO)₆(PCO)₂ structure **26-6S**, lying 31.4 kcal mol⁻¹ (B3LYP) or 35.4 kcal mol⁻¹ (BP86) in energy above **26-1S**, has two different types of bridging PCO groups (Figure 5 and Table 5). One of the bridging PCO groups is a three-electron donor bridging μ -PCO group bonded to the Mn atoms solely through the phosphorus atom similar to the bridging μ -PCO groups in the two lowest energy Mn₂(CO)₈(PCO)₂ structures **28-1S** and **28-2S** (Figure 3). The other bridging PCO group is the same type of bridging η^2 - μ -PCO ligand found in **26-5S**. Like **26-5S** discussed above, the Mn–Mn bond distance of 2.811 Å (B3LYP) or 2.712 Å (BP86) in **26-6S** also can be interpreted as a formal single bond, thereby giving the Mn atom bonded to four terminal CO groups (the “left” Mn atom in Figure 5) the favored 18-electron configuration but the other Mn atom only a 16-electron configuration.

The Mn₂(CO)₆(PCO)₂ structure **26-7S**, lying 23.2 kcal mol⁻¹ (B3LYP) or 37.3 kcal mol⁻¹ (BP86) in energy above **26-1S**, has two bridging μ -PCO groups bonded to the Mn atoms solely through their phosphorus atoms similar to the bridging μ -PCO groups in the two lowest energy Mn₂(CO)₈(PCO)₂ structures **28-1S** and **28-2S** (Figure 5 and Table 5). The Mn–Mn distance of 3.048 Å (B3LYP) or 2.898 Å (BP86) suggests the formal single bond required to give one Mn atom the favored 18-electron configuration but the other Mn atom only a 16-electron configuration.

3.2.4 Mn₂(CO)₅(PCO)₂. Three singlet structures and one triplet structure were optimized for Mn₂(CO)₅(PCO)₂ (Figure 6 and Table 6). All four structures are genuine minima with no imaginary vibrational frequencies. In all four structures the carbonyl part of at least one PCO ligand has migrated to an Mn atom, leaving at least one phosphorus atom bridging the two Mn atoms. Thus these complexes may be more precisely designated as Mn₂(CO)₇P₂, except for **25-3S**, which is Mn₂(CO)₆(PCO)(P).

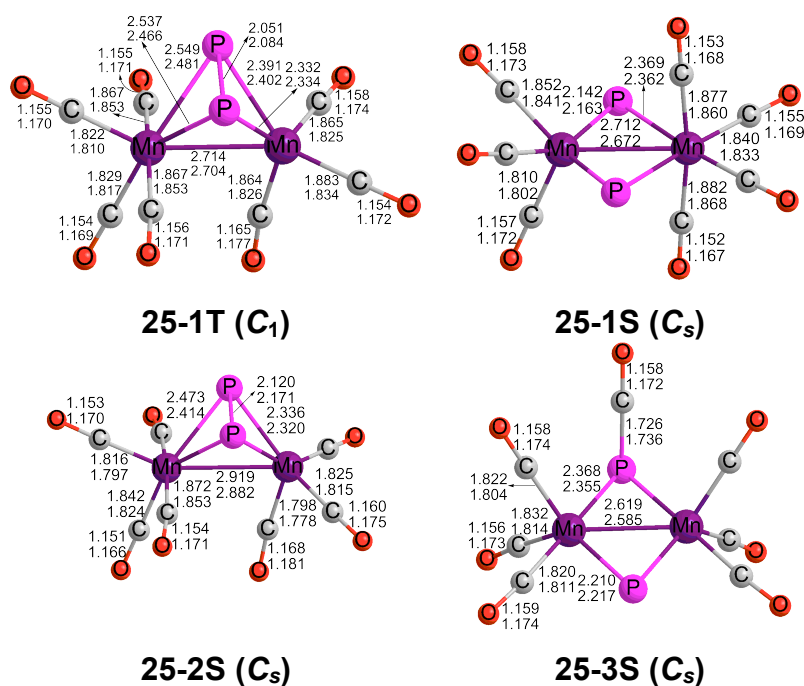


Figure 6. The optimized $\text{Mn}_2(\text{CO})_5(\text{PCO})_2$ structures. Bond distances are given in Å with the B3LYP values on top and the BP86 values on the bottom.

The B3LYP method predicts the lowest energy $\text{Mn}_2(\text{CO})_5(\text{PCO})_2$ structure to be the triplet **25-1T**, while the BP86 method predicts it to be the singlet **25-1S** (Figure 6 and Table 6). This is not surprising, since Reiher and coworkers have found that the B3LYP favors high-spin states, while the BP86 method favors low-spin states, with the true singlet-triplet splitting energies lying between the two predicted energies.^{34,35} Stability tests of the wavefunction have been performed for **25-1T** and **25-1S** at both the B3LYP and BP86 levels of theory. The results show that the wavefunctions of **25-1T** and **25-1S** are stable under the perturbations considered.

The $\text{Mn}_2(\text{CO})_5(\text{PCO})_2$ structure **25-1T** has the two phosphorus atoms generated by decarbonylation of the PCO ligands coupled to form a bridging $\mu\text{-P}_2$ unit with a P–P single bond distance of 2.051 Å (B3LYP) or 2.084 Å (BP86) (Figure 6 and Table 6). This P_2 ligand can be considered to be a four-electron donor providing two electrons for each Mn atom. The Mn=Mn bond distance for the triplet $\text{Mn}_2(\text{CO})_5(\text{PCO})_2$ structure **25-1T** is 2.714 Å (B3LYP) or 2.704 Å (BP86), which can be interpreted as formal double bond of the $\sigma + \frac{1}{2}\pi$ type. Such an Mn=Mn double bond in **25-1T** is similar to the Fe=Fe double bond in the experimentally known^{36,37} $(\eta^5\text{-C}_5\text{H}_5)_2\text{Fe}_2(\mu\text{-CO})_3$, in which the triplet spin state arises from the two unpaired electrons reside in the two orthogonal π

“half-bonds.” The Mn=Mn double bond gives each Mn atom in **25-1T** the favored 18-electron configuration with a formal positive charge on the Mn(CO)₄ manganese and a formal negative charge on the Mn(CO)₃ manganese.

Table 6 Total energies (E in Hartree), relative energies with and without ZPVE corrections (ΔE and ΔE_{ZPVE} in kcal mol⁻¹), and spin expectation values $\langle S^2 \rangle$ for the Mn₂(CO)₅(PCO) structures. None of the structures has any imaginary vibrational frequencies.

		25-1T (C ₁)	25-1S (C _s)	25-2S (C _s)	25-3S (C _s)
B3LYP	-E	3778.33255	3778.32235	3778.33113	3778.31657
	ΔE	0.0	6.4	0.9	10.0
	ΔE_{ZPVE}	0.0	7.6	1.7	11.2
	$\langle S^2 \rangle$	2.06	0.00	0.00	0.00
BP86	-E	3778.84087	3778.84618	3778.84365	3778.83202
	ΔE	0.0	-3.3	-1.7	5.6
	ΔE_{ZPVE}	0.0	-2.5	-1.1	6.4
	$\langle S^2 \rangle$	2.02	0.00	0.00	0.00

The relative energy of the singlet Mn₂(CO)₅(PCO)₂ structure **25-1S** should be close to that of **25-1T**, since the B3LYP method predicts **25-1S** to lie 6.4 kcal mol⁻¹ above **25-1T**, whereas the BP86 method predicts **25-1S** to lie 3.3 kcal mol⁻¹ below **25-1T** (Figure 6 and Table 6). Structure **25-1S** has two isolated phosphorus atoms bridging the manganese atoms, each acting as a three-electron donor to the central Mn₂ unit. The Mn–Mn distance of 2.712 Å (B3LYP) or 2.672 Å (BP86) suggests a short dative single bond from the Mn(CO)₄ manganese to the Mn(CO)₃ manganese. This gives each Mn atom in **25-1S** the favored 18-electron configuration.

The Mn₂(CO)₅(PCO)₂ structure **25-2S** lies only 0.9 kcal mol⁻¹ above **25-1T** (B3LYP) or 1.7 kcal mol⁻¹ (BP86) below **25-1T**, indicating these two structures to be almost degenerate in energy (Figure 6 and Table 6). Structure **25-2S** is an Mn₂(CO)₇(μ -P₂) structure in which the two phosphorus atoms generated by decarbonylation of the PCO ligands have coupled to form a bridging μ -P₂ unit with a P–P single bond distance of 2.120 Å (B3LYP) or 2.171 Å (BP86). The μ -P₂ ligand can be considered to be a four-electron donor providing two electrons for each Mn atom. The Mn–Mn distance of 2.919 Å (B3LYP) or 2.882 Å (BP86) in **25-2S** can be interpreted as a formal single bond. This gives the Mn atom bearing four CO groups the favored 18-electron configuration, but the Mn atom bearing three CO groups only a 16-electron configuration.

The $\text{Mn}_2(\text{CO})_5(\text{PCO})_2$ structure **25-3S**, lying $10.0 \text{ kcal mol}^{-1}$ (B3LYP) above **25-1T** or $5.6 \text{ kcal mol}^{-1}$ (BP86) below **25-1T**, is an $\text{Mn}_2(\text{CO})_6(\mu\text{-PCO})(\mu\text{-P})$ structure with one three-electron donor bridging $\mu\text{-PCO}$ group and one three-electron donor bridging $\mu\text{-P}$ group (Figure 6 and Table 6). The Mn=Mn distance of 2.619 \AA (B3LYP) or 2.585 \AA (BP86) is at least $\sim 0.1 \text{ \AA}$ shorter than any of the Mn–Mn distances in the other $\text{Mn}_2(\text{CO})_5(\text{PCO})_2$ structures suggested to be formal single bonds. This suggests the formal Mn=Mn double bond in **25-3S** required to give each Mn atom the favored 18-electron configuration.

3.3. Dissociation Energies

The predicted energies for dissociation of one CO group from the lowest energy singlet mononuclear $\text{Mn}(\text{CO})_m(\text{PCO})$ and binuclear $\text{Mn}_2(\text{CO})_n(\text{PCO})_2$ structures according to the following equations range from 15 to 45 kcal mol^{-1} (Table 7):



Thus the CO dissociation energy of $\text{Mn}(\text{CO})_5(\text{PCO})$ is predicted by the BP86 method to be $30.1 \text{ kcal mol}^{-1}$ (BP86), while the CO dissociation energy of $\text{Mn}(\text{CO})_4(\text{PCO})$ is predicted to be $26.7 \text{ kcal mol}^{-1}$ (B3LYP) or $32.6 \text{ kcal mol}^{-1}$ (BP86). These values are comparable with the known experimental carbonyl dissociation energies³⁸ of 27 kcal mol^{-1} for $\text{Ni}(\text{CO})_4$, 37 kcal mol^{-1} for $\text{Cr}(\text{CO})_6$ and 41 kcal mol^{-1} for $\text{Fe}(\text{CO})_5$. The dissociation energies required to remove one CO from the lowest-lying singlet binuclear structures of $\text{Mn}_2(\text{CO})_n(\text{PCO})_2$ ($n = 8, 7$) are similar at $20.7 \text{ kcal mol}^{-1}$ ($n = 8$) and $12.9 \text{ kcal mol}^{-1}$ ($n = 7$), respectively. However, the CO dissociation energy from $\text{Mn}_2(\text{CO})_6(\text{PCO})_2$ to give $\text{Mn}_2(\text{CO})_5(\text{PCO})_2$ is significantly higher at $45.2 \text{ kcal mol}^{-1}$. These substantial dissociation energies show that the $\text{Mn}(\text{CO})_m(\text{PCO})$ ($m = 5, 4$) and $\text{Mn}_2(\text{CO})_n(\text{PCO})_2$ ($n = 8, 7, 6$) complexes are all viable with respect to CO loss.

Table 7. Dissociation energies (kcal mol^{-1}) for the successive removal of carbonyl groups from the lowest singlet mononuclear and binuclear phosphaketenyl manganese carbonyls.

	B3LYP	BP86
$\text{Mn}(\text{CO})_5(\text{PCO}) \rightarrow \text{Mn}(\text{CO})_4(\text{PCO}) + \text{CO}$	26.0	30.1
$\text{Mn}(\text{CO})_4(\text{PCO}) \rightarrow \text{Mn}(\text{CO})_3(\text{PCO}) + \text{CO}$	26.7	32.6
$\text{Mn}_2(\text{CO})_8(\text{PCO})_2 \rightarrow \text{Mn}_2(\text{CO})_7(\text{PCO})_2 + \text{CO}$	15.7	20.7
$\text{Mn}_2(\text{CO})_7(\text{PCO})_2 \rightarrow \text{Mn}_2(\text{CO})_6(\text{PCO})_2 + \text{CO}$	21.6	12.9
$\text{Mn}_2(\text{CO})_6(\text{PCO})_2 \rightarrow \text{Mn}_2(\text{CO})_5(\text{PCO})_2 + \text{CO}$	41.4	45.2

The predicted energies for dissociation of the lowest-lying singlet binuclear $\text{Mn}_2(\text{CO})_n(\text{PCO})_2$ compounds ($n = 8, 7, 6, 5$) into mononuclear fragments by the following reactions range from 32 to 68 kcal mol⁻¹ (Table 8):



These significantly endothermic dissociation energies confirm that at least the binuclear $\text{Mn}_2(\text{CO})_8(\text{PCO})_2$ and $\text{Mn}_2(\text{CO})_7(\text{PCO})_2$ structures are viable relative to dissociation into mononuclear complexes.

The disproportionation energies reported in Table 9 correspond to reactions of the following type:



The predicted disproportionation of $\text{Mn}_2(\text{CO})_7(\text{PCO})_2$ into $\text{Mn}_2(\text{CO})_8(\text{PCO})_2 + \text{Mn}_2(\text{CO})_6(\text{PCO})_2$ by -8 kcal mol⁻¹ (B3LYP) or 6 kcal mol⁻¹ (BP86) suggests that such disproportionation is essentially thermoneutral suggesting that the even the lowest energy $\text{Mn}_2(\text{CO})_7(\text{PCO})_2$ structure (actually the $\text{Mn}_2(\text{CO})_9(\mu\text{-P}_2)$ structure **27-1S**) is not viable towards such disproportionation. However, the disproportionation of the lowest energy $\text{Mn}_2(\text{CO})_6(\text{PCO})_2$ structure (actually the $\text{Mn}_2(\text{CO})_8(\mu\text{-P}_2)$ structure **26-1S**) into $\text{Mn}_2(\text{CO})_7(\text{PCO})_2 + \text{Mn}_2(\text{CO})_5(\text{PCO})_2$ is clearly endothermic, suggesting that $\text{Mn}_2(\text{CO})_6(\text{PCO})_2$ is viable with respect to such disproportionation.

Table 8 Energies (kcal mol⁻¹) for dissociation of the lowest energy binuclear $\text{Mn}_2(\text{CO})_n(\text{PCO})_2$ structures into two mononuclear fragments.

	B3LYP	BP86
$\text{Mn}_2(\text{CO})_8(\text{PCO})_2 \rightarrow \text{Mn}(\text{CO})_5(\text{PCO}) + \text{Mn}(\text{CO})_3(\text{PCO})$	32.9	38.3
$\text{Mn}_2(\text{CO})_8(\text{PCO})_2 \rightarrow \text{Mn}(\text{CO})_4(\text{PCO}) + \text{Mn}(\text{CO})_4(\text{PCO})$	32.2	35.8
$\text{Mn}_2(\text{CO})_7(\text{PCO})_2 \rightarrow \text{Mn}(\text{CO})_4(\text{PCO}) + \text{Mn}(\text{CO})_3(\text{PCO})$	43.2	47.7
$\text{Mn}_2(\text{CO})_6(\text{PCO})_2 \rightarrow \text{Mn}(\text{CO})_3(\text{PCO}) + \text{Mn}(\text{CO})_3(\text{PCO})$	48.3	67.4

Table 9 Energies (kcal mol⁻¹) for the disproportionation of the lowest energy $\text{Mn}_2(\text{CO})_n(\text{PCO})_2$ ($n = 7, 6$) structures into $\text{Mn}_2(\text{CO})_{n+1}(\text{PCO})_2 + \text{Mn}_2(\text{CO})_{n-1}(\text{PCO})_2$.

	B3LYP	BP86
$2\text{Mn}_2(\text{CO})_7(\text{PCO})_2 \rightarrow \text{Mn}_2(\text{CO})_8(\text{PCO})_2 + \text{Mn}_2(\text{CO})_6(\text{PCO})_2$	5.9	-7.7
$2\text{Mn}_2(\text{CO})_6(\text{PCO})_2 \rightarrow \text{Mn}_2(\text{CO})_7(\text{PCO})_2 + \text{Mn}_2(\text{CO})_5(\text{PCO})_2$	19.8	32.3

3.4. Natural Bond Orbital (NBO) Analysis

Table 10 reports the natural charges for the two manganese atoms, the Wiberg bond indices (WBIs) for the Mn-Mn and P-P bonds as well as the Mn-Mn and P-P distances for the singlet $\text{Mn}_2(\text{CO})_n(\text{PCO})_2$ complexes obtained by natural bonding orbital (NBO)³⁹ analysis using the Gaussian03 (C.02) program.⁴⁰

The WBI values for the Mn-Mn bonds predicted by the BP86 method are consistent with the bond orders suggested by the Mn-Mn distances, electron counting, and coordination geometries (Table 10). Previous studies⁴¹ on the WBIs of metal carbonyls such as $\text{Fe}_2(\text{CO})_9$ and $\text{Fe}_3(\text{CO})_{12}$ show the WBIs of transition metal-metal bonds to be relatively low compared with the formal bond orders, particularly when the metal-metal bonds are bridged by carbonyl groups. This is consistent with our observations on the WBIs of the Mn-Mn bonds in the $\text{Mn}_2(\text{CO})_n(\text{PCO})_2$ derivatives. Thus the WBIs for the Mn-Mn formal single bonds range from 0.05 to 0.19. The only $\text{Mn}_2(\text{CO})_n(\text{PCO})_2$ species with a formal Mn=Mn double bond is the $\text{Mn}_2(\text{CO})_6(\mu\text{-PCO})(\mu\text{-P})$ species **25-3S** which has a significantly higher WBI of 0.30 for the Mn=Mn interaction than any of the $\text{Mn}_2(\text{CO})_n(\text{PCO})_2$ species with formal Mn-Mn single bonds. The WBI values for the Mn...Mn interactions in the $\text{Mn}_2(\text{CO})_n(\text{PCO})_2$ species in which the manganese atoms are too far apart for a direct bond are less than 0.04 except for those in **26-3S** and **26-4S**, which are ~0.09 (Table 10).

For bonds between main group atoms such as sulfur and phosphorus the WBI values are numerically close to the actual formal bond order in contrast to transition metal-metal bonds. For the $\text{Mn}_2(\text{CO})_n(\text{PCO})_2$ derivatives discussed in this paper, this is also the case. Thus for the $\text{Mn}_2(\text{CO})_n(\text{PCO})_2$ derivatives with a short enough P-P distance to suggest a direct bond, namely the $\text{Mn}_2(\text{CO})_7(\mu\text{-P}_2)$ tetrahedrane species **27-1S**, **27-2S**, **26-1S**, **26-2S**, **26-3S**, **26-4S**, and **25-2S** with a predicted bonding P-P distances ranging from 2.002 Å to 2.171 Å, the WBI values range from 1.18 to 2.00 (Table 10). More specifically, the structures **27-1S**, **27-2S**, and **26-4S** with P=P double bond distances of ~2.01 Å have WBIs ranging from 1.84 to 2.00 close to the assumed bond order of 2. The WBI values for the formally non-bonding P...P interactions in the other $\text{Mn}_2(\text{CO})_n(\text{PCO})_2$ structures are all less than 0.32.

The natural atomic charges on the manganese atoms for all of the $\text{Mn}_2(\text{CO})_n(\text{PCO})_2$ structures are negative and the negative values increase when more CO and PCO ligands are connected directly to a manganese atom (Table 10). This suggests that the backbonding of the manganese d electrons into the antibonding orbitals of CO and PCO, although strong relative to most other ligands, is not sufficient to compensate

for all of the charge transfer from the forward σ -bonding. However, since the backbonding capabilities of CO and PCO are not the same, there is not a simple relationship between the manganese natural atomic charge and the number of ligands.

Table 10 The Wiberg bond indices (WBI) for the Mn–Mn bonds and P–P bonds and the natural atomic charges for the Mn and Mn atoms in the singlet binuclear complexes $\text{Mn}_2(\text{CO})_n(\text{PCO})_2$ ($n = 8, 7, 6, 5$) predicted by the BP86 method.

	Mn–Mn distance (in Å)	Mn–Mn Bond Order	WBI for Mn–Mn	P–P distance (in Å)	P–P Bond Order	WBI for P–P	Natural charge on Mn/Mn
28-1S	3.829	0	0.01	3.179	0	0.06	-0.95/-0.95
28-2S	3.814	0	0.01	3.179	0	0.05	-0.95/-0.95
28-3S	4.363	0	0.02	3.753	0	0.01	-0.91/-0.72
27-1S	4.642	0	0.04	2.002	2	2.00	-0.91/-1.04
27-2S	5.644	0	0.03	2.005	2	1.95	-0.84/-1.01
27-3S	2.642	1	0.11	3.215	0	0.06	-0.92/-0.92
27-4S	2.649	1	0.11	2.969	0	0.09	-0.91/-0.91
27-5S	3.799	0	0.04	3.014	0	0.10	-0.96/-0.54
27-6S	3.731	0	0.01	2.976	0	0.10	-0.50/-0.95
27-7S	2.919	1	0.12	3.820	0	0.07	-0.95/-0.74
27-8S	2.920	1	0.05	3.844	0	0.07	-0.95/-0.74
26-1S	2.764	1	0.16	2.067	>1	1.45	-0.91/-0.91
26-2S	2.782	1	0.14	2.101	>1	1.33	-0.93/-0.93
26-3S	4.298	0	0.09	2.053	>1	1.77	-0.86/-0.86
26-4S	6.060	0	0.09	2.012	2	1.84	-0.78/-0.78
26-5S	2.760	1	0.13	3.786	0	0.17	-0.70/-1.04
26-6S	2.712	1	0.15	3.870	0	0.10	-0.62/-1.00
26-7S	2.898	1	0.09	2.924	0	0.10	-0.71/-0.56
25-1S	2.672	1	0.14	3.639	0	0.32	-0.84/-1.08
25-2S	2.882	1	0.19	2.171	1	1.18	-0.81/-0.58
25-3S	2.585	2	0.30	3.765	0	0.16	-0.74/-0.74

3.5. Vibrational Frequencies

The predicted $\nu(\text{CO})$ and $\nu(\text{PCO})$ vibrational frequencies for the optimized $\text{Mn}(\text{CO})_n(\text{PCO})$ ($n = 5, 4, 3$) and $\text{Mn}_2(\text{CO})_n(\text{PCO})_2$ ($n = 8, 7, 6, 5$) structures predicted by the BP86 method are listed in Tables 11 and 12. The BP86 method was chosen since in other systems it is shown to predict more reliable $\nu(\text{CO})$ frequencies than the B3LYP method without requiring a scaling factor.^{42,43} The terminal $\nu(\text{CO})$ frequencies for the CO groups in all of the $\text{Mn}(\text{CO})_n(\text{PCO})$ and $\text{Mn}_2(\text{CO})_n(\text{PCO})_2$ structures fall in the expected range from 2097 to 1921 cm^{-1} . The bridging CO groups in **27-3S** and **27-4S** exhibit significantly lower $\nu(\text{CO})$ frequencies of 1888 and 1885 cm^{-1} , respectively, in accord with expectation.

Table 11 The $\nu(\text{CO})$, $\nu(\text{CO})_{\text{PCO}}$ and $\nu(\text{PC})_{\text{PCO}}$ vibrational frequencies of the mononuclear $\text{Mn}(\text{CO})_n(\text{PCO})$ ($n = 5, 4, 3$) derivatives using the BP86 method. Infrared intensities in km mol^{-1} are given in parentheses.

Structures	$\nu(\text{CO})$	$\nu(\text{CO})_{\text{PCO}}$	$\nu(\text{PC})_{\text{PCO}}$
15-1S	1994(670), 2007(1352), 2008(1217), 2028(10), 2089(115)	1936(589)	736(6)
15-2S	1993(634), 2022(1238), 2024(1135), 2047(24), 2097(312)	1641(72)	832(1)
14-1S	1969(910), 1981(1071), 1988(1119), 2058(163)	1951(386)	686(5)
14-2S	1968(919), 1989(372), 1999(1280), 2068(429)	1651(35)	874(21)
13-1S	1962(907), 1964(715), 2027(492)	1742(266)	767(1)
13-2S	1951(885), 1951(885), 2021(675)	1669(69)	941(97)
13-1T	1958(1900), 1982(878), 2039(250)	1934(537)	698(20)

The $\text{Mn}(\text{CO})_5(\text{PCO})$ structure **15-1S** with a P-bonded PCO group and its isomer **15-2S** with an O-bonded PCO group exhibit the distinctly different $\nu(\text{CO})_{\text{PCO}}$ frequencies of 1936 and 1641 cm^{-1} , respectively (Table 11). In the binuclear structures $\text{Mn}_2(\text{CO})_n(\text{PCO})_2$ the $\nu(\text{CO})$ frequencies in the usual bridging μ -PCO groups (bonded to the Mn atoms only through the phosphorus atoms) range from 1934 to 2000 cm^{-1} (Table 12). The $\nu(\text{CO})$ frequency for the end-to-end bridging η^2 - μ -PCO group forming Mn–P and Mn–O bonds in **28-3S** is lower at 1775 cm^{-1} . The $\nu(\text{CO})$ frequencies for the bridging η^2 - μ -PCO groups forming Mn–P and Mn–C bonds in **26-5S** and **26-6S** are somewhat higher, ranging from 1803 to 1826 cm^{-1} .

In the mononuclear $\text{Mn}(\text{CO})_n(\text{PCO})$ structures, the $\nu(\text{PC})$ frequencies for the usual P-bonded terminal PCO groups range from 686 to 736 cm^{-1} (Table 11). The $\nu(\text{PC})$ frequency increases to 767 cm^{-1} for the trihapto η^3 -PCO ligand in **13-1S**. The $\nu(\text{PC})$ frequencies become significantly higher at 832 and 941 cm^{-1} in **15-2S** and **13-2S** for the PCO groups bonded to the Mn atom through the oxygen atom. In the binuclear structures $\text{Mn}_2(\text{CO})_n(\text{PCO})_2$, the $\nu(\text{PC})$ frequencies for the usual bridging PCO groups bonded to the Mn atoms through only the phosphorus atom range from 636 to 695 cm^{-1} (Table 12). The $\nu(\text{PC})$ frequencies become lower for the bridging η^2 - μ -PCO groups forming Mn–P and Mn–C bonds in **26-5S** and **26-6S**; they range from 531 to 595 cm^{-1} . The $\nu(\text{PC})$ frequency increases to 801 cm^{-1} for the end-to-end bridging PCO group forming Mn–P and Mn–O bonds in **28-3S**.

Table 12. The $\nu(\text{CO})$, $\nu(\text{CO})_{\text{PCO}}$ and $\nu(\text{PC})_{\text{PCO}}$ frequencies of the binuclear $\text{Mn}_2(\text{CO})_n(\text{PCO})_2$ ($n = 8, 7, 6, 5$) derivatives (with the BP86 method). Infrared intensities are given in parentheses in km mol^{-1} . The bridging $\nu(\text{CO})$, $\nu(\text{CO})_{\text{PCO}}$ and $\nu(\text{PC})_{\text{PCO}}$ frequencies are in **bold** type.

Structures	$\nu(\text{CO})$	$\nu(\text{CO})_{\text{PCO}}$	$\nu(\text{PC})_{\text{PCO}}$
28-1S	1968(0), 1973(0), 1976(1699), 1986(631), 1994(0), 1997(2817), 2039(1248), 2068(0)	1952(111), 1962(0)	681(0), 681(11)
28-2S	1967(0), 1973(0), 1981(2058), 1986(631), 1991(1001), 1998(1498), 2039(1246), 2068(17)	1956(0), 1958(11)	679(11), 683(0)
28-3S	1974(48), 1979(801), 1981(854), 1989(743), 1997(1094), 2002(1302), 2047(968), 2073(141)	1775(429) , 1957(14)	690(0), 801(5)
27-1S	1956(630), 1961(973), 1975(436), 2006(648), 2015(988), 2016(1334), 2030(1262), 2035(0), 2090(310)		
27-2S	1967(909), 1979(863), 1985(398), 1998(701), 2006(951), 2007(1505), 2026(17), 2038(1628), 2083(269)		
27-3S	1888(333) , 1968(3), 1980(6), 1984(1685), 1992(1785), 2018(1974), 2050(62)	1954(0), 1961(259)	651(13), 667(7)
27-4S	1885(282) , 1949(3), 1979(0), 1988(875), 1996(2406), 2017(1986), 2051(92)	1965(0), 1966(270)	663(13), 672(12)
27-5S	1945(154), 1946(376), 1980(1406), 1990(1992), 1994(522), 2014(1309), 2061(230)	1959(265), 1970(12)	668(4), 691(6)
27-6S	1943(332), 1946(164), 1968(1), 1986(1359), 1992(284), 2016(1423), 2062(238)	1971(56), 1986(2176)	691(9), 695(2)
27-7S	1930(310), 1946(360), 1987(949), 1990(1270), 1996(714), 2009(1614), 2063(194)	1959(283), 1963(426)	643(35), 644(11)
27-8S	1929(392), 1946(321), 1985(727), 1994(72), 1996(2293), 2007(1468), 2064(185)	1961(445), 1961(243)	636(9), 647(20)
26-1S	1964(20), 1968(247), 1973(1028), 1983(1025), 1988(4), 1994(886), 2015(1979), 2060(323)		
26-2S	1918(280), 1967(101), 1981(194), 1983(1738), 1992(523), 2003(297), 2023(1888), 2063(322)		
26-3S	1969(372), 1972(33), 1973(1382), 1990(405), 1991(2109), 1994(225), 2034(1941), 2065(26)		
26-1T	1973(0), 1974(1755), 1977(160), 1992(427), 1994(1194), 2000(896), 2025(2229), 2064(42)		

26-4S	1973(0), 1974(1917), 1983(0), 1989(2335), 1990(889), 1992(0), 2033(2879), 2061(0)		
26-2T	1959(352), 1971(1307), 1972(215), 1977(64), 1982(1594), 1982(1284), 2019(1650), 2053(79)		
26-5S	1985(68), 1992(567), 1994(1665), 1999(594), 2019(1376), 2059(185)	1803(902), 1824(128)	531(1), 566(14)
26-6S	1951(296), 1988(945), 1989(1094), 1996(218), 2001(1892), 2056(280)	1826(564) , 1961(301)	595(36), 651(7)
26-7S	1935(211), 1943(126), 1953(836), 1954(27), 1999(1752), 2039(219)	1980(13), 2000(2342)	664(14), 672(14)
25-1T	1930(272), 1949(433), 1975(1196), 1976(1275), 1988(1264), 1995(249), 2049(630)		
25-1S	1971(184), 1971(393), 1992(1678), 1994(538), 2000(297), 2004(1858), 2055(153)		
25-2S	1921(245), 1943(551), 1976(1225), 1981(617), 1992(1489), 2002(289), 2056(639)		
25-3S	1952(473), 1957(0), 1965(37), 1968(1058), 1992(1429), 2000(2055), 2035(90)	1992(1429)	

4. Discussion

The recently developed successful syntheses of the phosphoethynolate anion, PCO^- use reactions of a phosphide monoanion $\{\text{P}^-\}$ generator such as NaPH_2 or K_3P_7 with carbon monoxide.^{2,7} The chemistry of binuclear phosphaketenyl manganese carbonyl derivatives derived from the PCO^- anion based on the predicted lowest energy structures suggests that this reaction sequence can be reversed. This means that the PCO ligand can transfer its CO group to the Mn atom thereby leaving a bare phosphide or diphosphide ligand to bridge the central Mn_2 unit. Thus initial loss of a CO group from the octacarbonyl $\text{Mn}_2(\text{CO})_8(\mu\text{-PCO})_2$ (**28-1S**) might be expected first to result in formation of a Mn–Mn bond to give $\text{Mn}_2(\text{CO})_6(\mu\text{-CO})(\mu\text{-PCO})_2$ (**27-3S**). However, this structure **27-3S** lies ~ 14 kcal/mol (B3LYP) or ~ 7 kcal/mol (BP86) above an isomeric $\text{Mn}_2(\text{CO})_9(\mu\text{-P}_2)$ structure **27-1S** in which the CO groups in both PCO ligands have migrated from phosphorus to manganese. For the more highly decarbonylated species, several $\text{Mn}_2(\text{CO})_{n+2}(\mu\text{-P}_2)$ isomers ($n = 6, 5$) are lower energy structures than their

$\text{Mn}_2(\text{CO})_n(\mu\text{-PCO})_2$ isomers with intact PCO ligands. Thus carbonyl migration from PCO ligands to manganese atoms appears to be an energetically favorable process.

Migration of a carbonyl group from a PCO ligand to a transition metal atom is expected to involve intermediates having dihapto $\eta^2\text{-}\mu\text{-PCO}$ ligands bonded to metal atoms through both their phosphorus and carbon atoms. Intermediates of this type are found in the $\text{Mn}_2(\text{CO})_6(\text{PCO})_2$ structures **26-5S** and **26-6S**, which, however, lie ~ 30 kcal/mol in energy above the lowest energy $\text{Mn}_2(\text{CO})_8(\mu\text{-P}_2)$ isomer **26-1S** (Figure 5 and Table 5). The essential features of this CO migration process are depicted in Figure 7 omitting for clarity the CO groups not undergoing migration. For example, in **26-5S** the two dihapto $\eta^2\text{-PCO}$ groups donate a total of six electrons to the central Mn_2 unit. However, in **25-1S** the combination of two new terminal CO groups and the two bridging phosphorus atoms donate ten electrons to the central Mn_2 unit. Thus carbonyl migration from PCO ligands to metal atoms can compensate for the unsaturation generated by loss of CO groups in a binuclear phosphaketanyl metal carbonyl. Note that for the $\text{Mn}_2(\text{CO})_n(\text{PCO})_2$ system no low energy structures having formal Mn-Mn bond orders greater than two are found. Thus carbonyl migration from PCO ligands to manganese in this system appears to be a lower energy process than formation of metal-metal multiple bonds.

The PCO^- ligand is the phosphorus analogue of the well-known isocyanate ligand NCO^- , which is one of the original ambidentate ligands, bonding to metal atoms either through its nitrogen atom or its oxygen atom. The phosphoethynolate anion PCO^- is an analogous ambidentate ligand,⁸ which can bond as a monohapto ligand to a metal atom either through its phosphorus or its oxygen atom. The P-bonded PCO^- can be considered formally as the phosphaketanyl ligand M-P=C=O whereas the O-bonded PCO^- ligand can be considered as the phosphoethynoxy ligand $\text{M-O-C}\equiv\text{P}$. The isomeric P-bonded phosphaketanyl $\text{Mn}(\text{CO})_n(\text{PCO})$ and O-bonded 2-phosphoethynoxy $\text{Mn}(\text{CO})_n(\text{OCP})$ structures are both found as **15-1S** and **15-2S**, respectively, for $n = 5$ and as **14-1S** and **14-2S**, respectively, for $n = 4$ (Figure 1 and Table 1). However, the 2-phosphoethynoxy structures **15-2S** and **14-2S** are predicted to lie ~ 28 to ~ 20 kcal mol⁻¹ in energy, respectively, above the isomeric phosphaketanyl structures **15-1S** and **14-1S**, respectively. This suggests that O-bonded 2-phosphoethynoxy structures are much less favorable than P-bonded phosphaketanyl structures. This is consistent with a recent spectroscopic and computational study on $\text{R}_3\text{E}(\text{PCO})/\text{R}_3\text{E}(\text{OCP})$ ($\text{R} = \text{Ph}, \text{}^i\text{Pr}$; $\text{E} = \text{Si}, \text{Ge}, \text{Sn}, \text{Pb}$) systems by Grützmacher and coworkers, who find the P-bonded phosphaketene isomers to be the thermodynamically preferred products.⁸ The phosphaketene and phosphoethynoxy

ligands are both linear but the angle at the ligating atom is bent rather than linear owing to the presence of stereochemically active lone pairs (Figure 8). For the $\text{Mn}(\text{CO})_n(\text{PCO})/\text{Mn}(\text{CO})_n(\text{OCP})$ isomer pairs this bending appears to be sharper for the P-bonded phosphaketenyl complexes than for the O-bonded phosphoethynoxy complexes. For example in the $\text{Mn}(\text{CO})_5(\text{PCO})$ structure **15-1S** the Mn–P–C angle is $\sim 98^\circ$ whereas in the isomeric $\text{Mn}(\text{CO})_5(\text{OCP})$ structure **15-2S** the Mn–O–C angle widens to $\sim 124^\circ$. No examples of the less favorable O-bonded phosphoethynoxy structures $\text{Mn}_2(\text{CO})_n(\text{OCP})_2$ were found for the binuclear derivatives. Furthermore, the phosphaketenyl ligands in the low energy $\text{Mn}_2(\text{CO})_n(\text{PCO})_2$ structures were always bridging ligands.

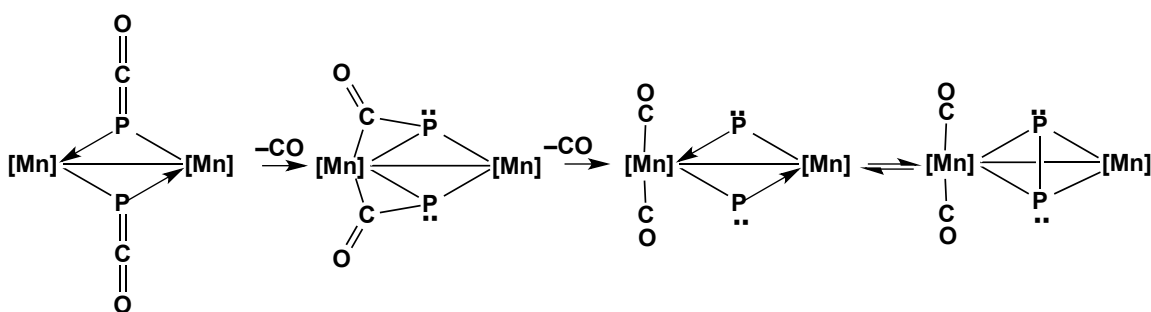


Figure 7. The migration of CO groups bonded to phosphorus in bridging PCO ligands to manganese in the $\text{Mn}_2(\text{CO})_n(\text{PCO})$ derivatives. The CO groups not undergoing migration are omitted for clarity.



Figure 8. The phosphaketenyl P-bonded and phosphoethynoxy O-bonded coordination modes of the PCO^- ligand.

The P-bonded (phosphaketenyl) PCO^- ligand has a formal C=O double bond whereas the O-bonded (phosphoethynoxy) PCO^- ligand has a formal C–O single bond (Figure 8). This is consistent with the predicted $\nu(\text{CO})_{\text{PCO}}$ frequency of 1936 cm^{-1} for the phosphaketenyl derivative $\text{Mn}(\text{CO})_5(\text{PCO})$ (**15-1S**) being higher than the 1641 cm^{-1} $\nu(\text{CO})_{\text{PCO}}$ frequency for the phosphoethynoxy derivative $\text{Mn}(\text{CO})_5(\text{OCP})$ (**15-2S**). The lower experimental $\nu(\text{CO})_{\text{PCO}}$ frequency of 1860 cm^{-1} in tetrahydrofuran for the experimentally known³ (triphos)Re(CO)₂(PCO) relative to the predicted value for **15-1S** can be a consequence of the replacement of three CO groups in **15-1S** by the weaker back-bonding tritertiary phosphine ligand. Similarly the P-bonded (phosphaketenyl)

PCO⁻ ligand has a formal P=C double bond, whereas the O-bonded (phosphaethynoxy) PCO⁻ ligand has a formal P≡C triple bond. This is consistent with the predicted $\nu(\text{PC})_{\text{PCO}}$ frequency of 736 cm⁻¹ for **15-1S** being lower than the 832 cm⁻¹ $\nu(\text{PC})_{\text{PCO}}$ frequency for the O-bonded Mn(CO)₅(COP) derivative **15-2S**. In the binuclear Mn₂(CO)_n(PCO)₂ derivatives the $\nu(\text{CO})_{\text{PCO}}$ frequencies for the usual monohapto bridging μ -PCO groups bonded to the metals only through the phosphorus atoms range from 1952 to 2000 cm⁻¹, which is only slightly higher than the terminal $\nu(\text{CO})_{\text{PCO}}$ frequency of 1936 cm⁻¹ in the mononuclear Mn(CO)₅(PCO). The predicted $\nu(\text{CO})_{\text{PCO}}$ frequencies for the dihapto bridging η^2 - μ -CO groups in the Mn₂(CO)₆(η^2 - μ -PCO)₂ structures **26-5S** and **26-6S** are significantly lower, ranging from 1803 to 1826 cm⁻¹. The CO groups in the dihapto η^2 - μ -PCO ligands bridging an Mn–P bond in **26-5S** and **26-6S** are analogous to the frequent examples of CO groups bridging metal-metal bonds in polynuclear metal carbonyl chemistry. The CO groups in the more frequently encountered bridging μ -PCO ligands bonded to metal atoms only through their phosphorus atoms are analogous to terminal CO groups in metal carbonyl chemistry. Therefore it is not surprising that the $\nu(\text{CO})$ frequencies for the dihapto bridging η^2 - μ -PCO ligands in **26-5S** and **26-2S** are lower by ~150 cm⁻¹ than those for bridging μ -PCO groups bonded to the metals only through the phosphorus atoms.

5. Summary

The phosphaethynolate anion, PCO⁻, like the analogous isocyanate anion, NCO⁻ is predicted to be an ambidentate ligand in manganese carbonyl chemistry with isomeric P-bonded phosphaketanyl Mn(CO)_n(PCO) and O-bonded phosphaethynoxy Mn(CO)_n(OCP) structures ($n = 5, 4$) both being stationary points without imaginary vibrational frequencies. However, the O-bonded Mn(CO)_n(OCP) structures ($n = 5, 4$) are found to lie ~20 to 28 kcal mol⁻¹ in energy above the isomeric P-bonded Mn(CO)_n(PCO) structures. The lowest energy structure for the tricarbonyl Mn(CO)₃(PCO) is a singlet structure with an unusual trihapto η^3 -PCO ligand. However, higher energy Mn(CO)₃(PCO) structures with a P-bonded phosphaketanyl ligand and tetrahedral Mn coordination and with an O-bonded phosphaethynoxy ligand are also found.

For the binuclear systems the low-energy Mn₂(CO)₈(PCO)₂ structures are singlet spin state structures having two bridging P-bonded phosphaketanyl μ -PCO ligands without a direct Mn–Mn bond. Carbonyl loss from Mn₂(CO)₈(μ -PCO)₂ is predicted to lead to migration of CO groups from phosphorus to manganese resulting in

$\text{Mn}_2(\text{CO})_{n+2}(\mu\text{-P}_2)$ structures with bridging diphosphido groups as the lowest energy $\text{Mn}_2(\text{CO})_n(\text{PCO})_2$ isomers ($n = 7, 6, 5$). Isomeric $\text{Mn}_2(\text{CO})_6(\text{PCO})_2$ structures with dihapto bridging $\eta^2\text{-}\mu\text{-PCO}$ ligands lying ~ 30 kcal/mol above the lowest energy $\text{Mn}_2(\text{CO})_8(\mu\text{-P}_2)$ isomer are also found representing intermediates in the migration of CO groups from phosphorus to manganese.

Acknowledgments. We are indebted to the National Natural Science Foundation (21273082) of China, as well as the U. S. National Science Foundation (Grants CHE-1057466 and CHE-1361178) for financial support of this research.

Supporting Information. Tables S1 to S3: Optimized coordinates of $\text{Mn}_2(\text{CO})_8(\text{PCO})_2$; Tables S4 to S11: Optimized coordinates of $\text{Mn}_2(\text{CO})_7(\text{PCO})_2$; Tables S12 to S20: Optimized coordinates of $\text{Mn}_2(\text{CO})_6(\text{PCO})_2$; Tables S21 to S24: Optimized coordinates of $\text{Mn}_2(\text{CO})_5(\text{PCO})_2$; Tables S25 and S26: Optimized coordinates of $\text{Mn}(\text{CO})_5(\text{PCO})$; Tables S27 and S28: Optimized coordinates of $\text{Mn}(\text{CO})_4(\text{PCO})$; Tables S28 to S30: Optimized coordinates of $\text{Mn}(\text{CO})_3(\text{PCO})$; Tables S32 to S34: Harmonic vibrational frequencies (cm^{-1}) and IR intensities (km/mol) of $\text{Mn}_2(\text{CO})_8(\text{PCO})_2$; Tables S35 to S42: Harmonic vibrational frequencies (cm^{-1}) and IR intensities (km/mol) of $\text{Mn}_2(\text{CO})_7(\text{PCO})_2$; Tables S43 to S51: Harmonic vibrational frequencies (cm^{-1}) and IR intensities (km/mol) of $\text{Mn}_2(\text{CO})_6(\text{PCO})_2$; Tables S52 to S55: Harmonic vibrational frequencies (cm^{-1}) and IR intensities (km/mol) of $\text{Mn}_2(\text{CO})_5(\text{PCO})_2$; Tables S56 and S57: Harmonic vibrational frequencies (cm^{-1}) and IR intensities (km/mol) of $\text{Mn}(\text{CO})_5(\text{PCO})$; Tables S58 and S59: Harmonic vibrational frequencies (cm^{-1}) and IR intensities (km/mol) of $\text{Mn}(\text{CO})_4(\text{PCO})$; Tables S60 to S62: Harmonic vibrational frequencies (cm^{-1}) and IR intensities (km/mol) of $\text{Mn}(\text{CO})_3(\text{PCO})$; Complete Gaussian 09 reference (Reference 25).

Literature References

- (1) Becker, G.; Schwarz, W.; Seidler, N.; Westerhausen, M. *Z. Anorg. Allgem. Chem.*
- (2) Puschmann, F. F.; Stein, D.; Heift, D.; Hendriksen, C.; Gal, Z. A.; Grützmacher, H.-F.; Grützmacher, H. *Angew. Chem. Int. Ed.* **2011**, *50*, 8420.
- (3) Alidori, S.; Heift, D.; Santiso-Quinones, G.; Benkő, Z.; Grützmacher, H.; Caporali, M.; Gonsalvi, L.; Rossin, A.; Peruzzini, M. *Chem. Eur. J.* **2012**, *18*, 14805.
- (4) Heift, D.; Benkő, Z.; Grützmacher, H. *Dalton Trans.* **2014**, *43*, 831.
- (5) Chen, X.; Alidori, S.; Puschmann, F. F.; Santiso-Quinones, G.; Benkő, Z.; Li, Z.; Becker, G.; Grützmacher, H.-F.; Grützmacher, H. *Angew. Chem. Int. Ed.* **2014**, *53*, 1641.
- (6) Tondreau, A. M.; Benkő, Z.; Harmer, J. R.; Grützmacher, H. *Chem. Sci.* **2014**, *5*, 1545.
- (7) Jupp, A. R.; Goicoechea, J. M. *Angew. Chem. Int. Ed.* **2013**, *52*, 10064.
- (8) Heift, D.; Benkő, Z.; Grützmacher, H. *Dalton Trans.* **2014**, *43*, 5920.
- (9) Ziegler T.; Autschbach, J. *Chem. Rev.* **2005**, *105*, 2695.
- (10) Bühl, M.; Kabrede, H. *J. Chem. Theory Comput.* **2006**, *2*, 1282.
- (11) Brynda, M.; Gagliardi, L.; Widmark, P. O.; Power, P. P.; Roos, B. O. *Angew. Chem. Int. Ed.* **2006**, *45*, 3804.
- (12) Sieffert, N.; Bühl, M. *J. Am. Chem. Soc.* **2010**, *132*, 8056.
- (13) Schyman, P.; Lai, W.; Chen, H.; Wang, Y.; Shaik, S. *J. Am. Chem. Soc.* **2011**, *133*, 7977.
- (14) Adams, R. D.; Pearl, W. C.; Wong, Y. O.; Zhang, Q.; Hall, M. B.; Walensky, J. R. *J. Am. Chem. Soc.* **2011**, *133*, 12994.
- (15) Lonsdale, R.; Olah, J.; Mulholland, A. J.; Harvey, J. N. *J. Am. Chem. Soc.* **2011**, *133*, 15464.
- (16) Becke, A. D. *Phys. Rev. A* **1988**, *38*, 3098.
- (17) Lee, C.; Yang, W.; Parr, R. G. *Phys. Rev. B* **1988**, *37*, 785.
- (18) Becke, A. D. *Phys. Rev. A* **1988**, *38*, 3098.
- (19) Perdew, J. P. *Phys. Rev. B* **1986**, *33*, 8822.
- (20) Dunning, T. H. *J. Chem. Phys.* **1970**, *53*, 2823.
- (21) Huzinaga, S. *J. Chem. Phys.* **1965**, *42*, 1293.
- (22) Wachters, A. J. H. *J. Chem. Phys.* **1970**, *52*, 1033.
- (23) Hood, D. M.; Pitzer, R. M.; Schaefer, H. F. *J. Chem. Phys.* **1979**, *71*, 705.

- (24) Narendrapurapu, B. S.; Richardson, N. A.; Copan, A. V.; Estep, M. L.; Yang, Z.; Schaefer, H. F. *J. Chem. Theor. Comput.*, **2013**, *9*, 2930.
- (25) Frisch, M. J. *et al.* Gaussian 09, Revision A.02; Gaussian, Inc., Wallingford CT, 2009.
- (26) Papas, B. N.; Schaefer, H. F. *J. Mol. Struct.*, **2006**, *768*, 175.
- (27) LaPlaca, S. J.; Ibers, J. A.; Hamilton, W. C. *J. Am. Chem. Soc.* **1964**, *86*, 2288.
- (28) LaPlaca, S. J.; Hamilton, W. C.; Ibers, J. A. *Inorg. Chem.* **1964**, *3*, 1491.
- (29) Liu, X.-m.; Wang, C.-y.; Li, Q.-s.; Xie, Y.; King, R. B.; Schaefer, H. F. *Dalton Trans.* **2009**, 3774.
- (30) Bennett, M. J.; Graham, W. A. G.; Hoyano, J. K.; Hutcheon, W. L. *J. Am. Chem. Soc.* **1972**, *94*, 6232.
- (31) Masciochi, N.; Sironi, A.; D'Alfonso, G. *J. Am. Chem. Soc.* **1990**, *112*, 9395.
- (32) Dahl, L. F.; Rundle, R. E. *Acta Crystallogr.* **1963**, *16*, 419.
- (33) Martin, M.; Rees, B.; Mitschler, A. *Acta Crystallogr.* **1982**, *38B*, 6.
- (34) Reiher, M.; Salomon, O.; Hess, B. A. *Theor. Chem. Acc.* **2001**, *107*, 48.
- (35) Salomon, O.; Reiher, M.; Hess, B. A. *J. Chem. Phys.* **2002**, *117*, 4729.
- (36) Caspar, J. V.; Meyer, T. J. *J. Am. Chem. Soc.* **1980**, *102*, 7794.
- (37) Hepp, A. F.; Blaha, J. P.; Lewis, C.; Wrighton, M. S. *Organometallics* **1984**, *3*, 174.
- (38) Sunderlin, L. S.; Wang, D.; Squires, R. R. *J. Am. Chem. Soc.*, **1993**, *115*, 12060.
- (39) Reed, A. E.; Curtiss, L. A.; Weinhold, F. *Chem. Rev.* **1988**, *88*, 899.
- (40) Frisch, M. J. *et al.* Gaussian 03, Revisions E.01 and C.02, Gaussian, Inc., Wallingford, CT (2004).
- (41) Wang, H.; Xie, Y.; King, R. B.; Schaefer, H. F. *J. Am. Chem. Soc.* **2006**, *128*, 11376.
- (42) Silaghi-Dumitrescu, I.; Bitterwolf, T. E.; King, R. B. *J. Am. Chem. Soc.* **2006**, *128*, 5342.
- (43) Jonas, V.; Thiel, W. *J. Chem. Phys.* **1995**, *102*, 8474.

11/14

Table of Contents Entry

Carbonyl Migration from Phosphorus to the Metal in Binuclear Phosphaketenyl Metal Carbonyl Complexes to Give Bridging Diphosphido Complexes

Wenjun Lü, Chaoyang Wang, Qiong Luo,*
Qian-shu Li, Yaoming Xie,
R. Bruce King,* and Henry F. Schaefer

Carbonyl groups from bridging phosphaketenyl ligands in $\text{Mn}_2(\text{CO})_8(\mu\text{-PCO})_2$ are predicted to migrate from phosphorus to manganese upon decarbonylation, giving the diphosphido $\text{Mn}_2(\text{CO})_{n+2}(\mu\text{-P}_2)$ derivatives via $\text{Mn}_2(\text{CO})_n(\text{PCO})_2$ intermediates with one or two bridging dihapto $\eta^2\text{-}\mu\text{-PCO}$ ligands.

